PAPER Special Section on Superconducting High-frequency Devices

Design of a Miniaturized Superconducting Bandpass Filter by Evaluating the Kinetic Inductance in the *K*-Inverter

Haruichi KANAYA[†a)], **Koji KAWAKAMI**[†], ***and*** **Keiji YOSHIDA**[†], ***Members***

SUMMARY We propose a design theory of the miniaturized high temperature superconducting (HTS) coplanar waveguide (CPW) bandpass filter (BPF), which is composed of meanderline quarter-wavelength resonator, *J*- and *K*-inverters. The *J*- and *K*-inverters are realized by using interdigital gap and meander-shape inductor. To evaluate the kinetic inductance of the *K*-inverter, we fabricate the YBCO resonator connected with *K*-inverters and redesigned the YBCO filter parameters. Finally, we designed and fabricated the YBCO CPW quarter-wavelength resonator BPF by taking account of the kinetic inductance of the *K*-inverter. The experimental results are in agreement with the design parameters.

key words: *HTS passive device, bandpass filter, quarter-wavelength resonator, meander line, coplanar waveguide*

1. Introduction

High temperature superconducting (HTS) passive devices have an extremely high potential in the wireless base station systems, because of significant low insertion loss and high sensitivity. There are many reports on microstrip bandpass filter (BPF) [1]–[3], and HTS BPF based cryogenic receiver front-ends [4]. In order to reduce the cooling cost of the HTS filter subsystem, it is very important to miniaturize the HTS devices. A coplanar waveguide (CPW) is coated before patterning only one side of the substrate because the signal line and earth conductor exist only on the same side, and it is easy to make size reduction because the characteristic impedance of the transmission line depends only on the ratio of strip to slot width and dose not depend on the thickness of the substrate. So, the CPW is more advantageous than the microstrip structure.

In our previous studies [5]–[7], we designed the miniaturized cross-coupled CPW BPF by using highly packed meanderline half-wavelength ($\lambda/2$) resonators and interdigital gaps (*J*-inverters). In this paper, for further miniaturization, we designed and tested quarter wavelength ($\lambda/4$) resonator BPF by using interdigital gaps and meander-shape inductors (*K*-inviters). However, the effect of the kinetic inductance of HTS appears conspicuously and quality factor becomes lower because the microwave current concentrates on the narrow meander inductor. The effect of the kinetic inductance changes the bandwidth of the BPF (see Eqs. (3)), and lower quality factor causes the insertion loss in the pass band. However, most important problem for the narrow band HTS BPF is the difference of the bandwidth between the design parameter and experimental result.

In order to take account of the kinetic inductance in the *K*-inverter, we fabricate the YBCO resonator connected with *K*-inverters and redesigned the YBCO filter parameters by using the experimental results. The prototype YBCO miniaturized BPF (center frequency = 10 GHz, 2-pole, bandwidth=1.5%), which includes the kinetic inductance of the *K*-inverter, is also tested in cryogenic temperature. We show that the experimental results are in agreement with the design parameters.

2. Design of Chebyshev Quarter-Wavelength Resonator CPW Bandpass Filter

2.1 Design Parameters of the $\lambda/4$ Resonator BPF

Figure 1(a) shows the lumped element circuit model of the BPF [8]. Series resonator (jX_0) is transformed into the shunt resonator (jB_0) by interconnecting two *J*-inverters as shown in Fig. 1(b). Figure 1(c) and Fig. 1(d) shows the equivalent

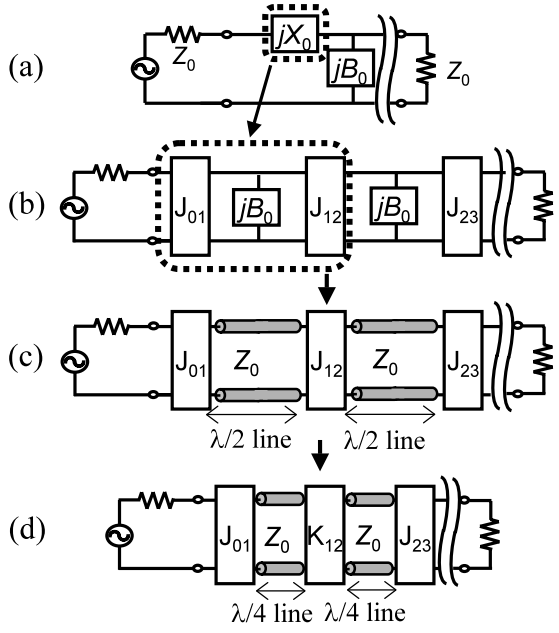

Fig. 1 Lumped element circuit model of the BPF (a), circuit model composed of the shunt resonators and *J*-inverters (b), equivalent circuit model of the BPF with $\lambda/2$ resonators (b) and $\lambda/4$ resonators (c).

Manuscript received June 20, 2005.
Manuscript revised August 23, 2005.

[†]The authors are with the Department of Electronics, Graduate School of Information Science and Electrical Engineering, Kyushu University, Fukuoka-shi, 812-8581 Japan.
a) E-mail: kanaya@ed.kyushu-u.ac.jp

DOI: 10.1093/ietele/e89–c.2.145

circuit model of the BPF with $\lambda/2$ resonators and $\lambda/4$ resonators, respectively [9]. In Fig. 1(d), the $\lambda/4$ resonator is connected with the J-and K-inverters, so that total length of the BPF is almost as half as that of the $\lambda/2$ resonator BPF.

The design parameters of the Chebyshev type $\lambda/2$ resonator BPF are given by [8]

$$\begin{cases} J_{01} = \sqrt{w}\sqrt{\dfrac{Y_0 b_0}{g_0 g_1}} \\ J_{i,i+1} = w\sqrt{\dfrac{b_0 b_0}{g_i g_{i+1}}} \quad (i = 1, 2, \cdots, n-1) \\ J_{n,n+1} = \sqrt{w}\sqrt{\dfrac{Y_0 b_0}{g_n g_{n+1}}} \\ b_0 = \dfrac{\omega_0}{2}\dfrac{\partial B_0}{\partial \omega}\Big|_{\omega=\omega_0} = \dfrac{\pi}{4}Y_0 = \dfrac{\pi}{4}\dfrac{1}{Z_0} \end{cases}, \tag{1}$$

Where, w and g_i are the fractional bandwidth and element values of Chebyshev BPF, respectively. b_0 is the suseptance slope parameter of the shunt resonator (jB_0) at the resonant frequency (ω_0) (see Fig. 1(a)).

In order to realize the miniaturized BPF, these resonators are modified and bended to the meanderline structures. The bended resonators change the slope parameters because of the interconnection between the resonators. The reactance slope parameter (x_i) and suseptance slope parameter (b_j) of the i-th resonator (jX_i) and j-th resonator (jB_j) can be calculated and given by

$$\begin{cases} x_i = \dfrac{\omega_0}{2}\dfrac{\partial X_i}{\partial \omega}\Big|_{\omega=\omega_0} = \dfrac{\pi}{4}Z_i \\ b_j = \dfrac{\omega_0}{2}\dfrac{\partial B_j}{\partial \omega}\Big|_{\omega=\omega_0} = \dfrac{\pi}{4}Y_j \end{cases}, \tag{2}$$

where, Z_i and Y_j=$(1/Z_j)$ are characteristic impedance and characteristic admittance, respectively.

The design parameters of the even pole number $\lambda/4$ resonator BPF are given by

$$\begin{cases} J_{01} = \sqrt{w}\sqrt{\dfrac{Y_0 b_1}{g_0 g_1}} = \dfrac{\pi}{4}\sqrt{w}\sqrt{\dfrac{1}{g_0 g_1 x_1 Z_0}} \\ K_{i,i+1} = w\sqrt{\dfrac{x_i x_{i+1}}{g_i g_{i+1}}} = \left(\dfrac{\pi}{4}\right)^2 w\sqrt{\dfrac{1}{g_i g_{i+1} b_i b_{i+1}}} \\ \quad (i = 1, 3, \cdots, 2n-1) \\ J_{i,i+1} = w\sqrt{\dfrac{b_i b_{i+1}}{g_i g_{i+1}}} = \left(\dfrac{\pi}{4}\right)^2 w\sqrt{\dfrac{1}{g_i g_{i+1} x_i x_{i+1}}} \\ \quad (i = 2, 4, \cdots, 2n-2) \\ J_{n,n+1} = \sqrt{w}\sqrt{\dfrac{Y_0 b_n}{g_n g_{n+1}}} = \dfrac{\pi}{4}\sqrt{w}\sqrt{\dfrac{1}{g_n g_{n+1} x_n Z_0}} \end{cases}. \tag{3}$$

We can see K- and J-inverters change the bandwidth (w) of the BPF.

2.2 Design of the K-Inverter and J-Inverter

The exact inverters, and slope parameters of the $\lambda/4$ resonators are calculated by using the electromagnetic field simulator (EM-simulator) (Agilent, ADS2004A). Figure 2 shows the layout of the K-inverters. They are realized by using meanderline inductors. The YBCO film is approximated as the perfect conductor and the thickness of the MgO (ε_r=9.6) substrate is 500 μm. The width of the signal line and gap interval is 60 μm and 26 μm (characteristic impedance =50 Ω), respectively (see Fig. 2). In the figure, d_m and n is the length and bending number of the K-inverters. In the previous paper, we found that K values are saturated even d_m becomes longer [9]. In this paper, in order to design the BPFs, which have a lot of pole number, fractional bandwidth and so on, we modified the shape of the inverters, which is adjustable in wide range. In order to suppress the interference of the magnetic field around the meander inductor, the gap (s_m) is stretched from 15 μm, to 60 μm (see Fig. 2).

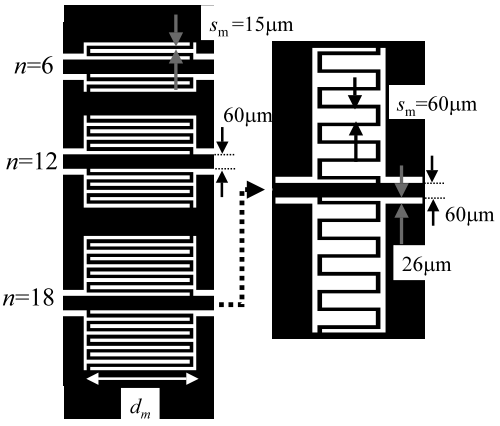

Fig. 2 Layout of the meander inductor (K-inverter). d_m, s_m and n is the length, gap width and bending numbers of the K-inverters, respectively.

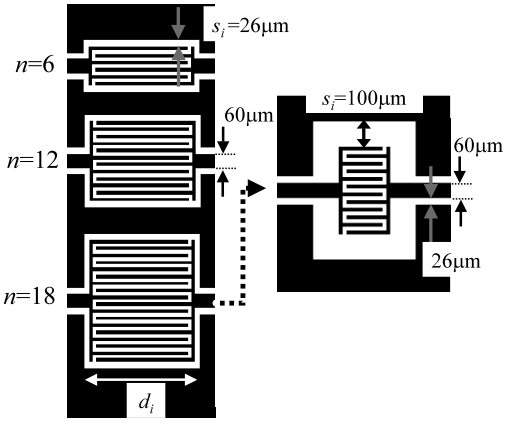

Fig. 3 Layout of the interdigital capacitor (J-inverter). d_i, s_i and n is the length, gap width and bending numbers of the J-inverters, respectively.

Figure 3 shows the layout of the J-inverters. In the figure, d_i and n is the length and finger numbers of the J-inverters, respectively. We also confirmed that J values are saturated even d_i becomes longer [9]. In order to suppress the effect of the shunt capacitance between signal line and earth conductor, the gap (s_i) is stretched from 26 μm, to

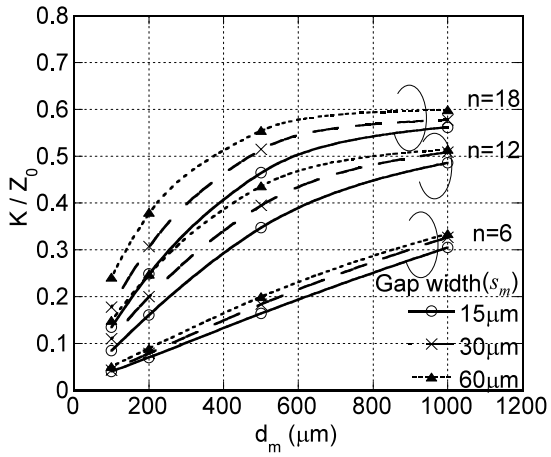

Fig. 4 EM-simulation results of the d_m and s_m dependences on K-inverters.

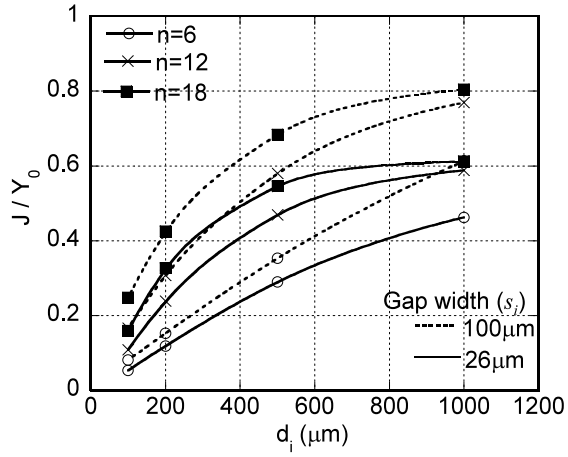

Fig. 5 EM-simulation results of the d_i and s_i dependences on J-inverters.

100 μm (see Fig. 3).

Figure 4 shows the EM-simulation results of the d_m and s_m dependence on K-inverters. K values are normalized by Z_0 (=50 Ω). K/Z_0 are both increased by stretching the gap, but are saturating in large d_m regions. Although large K-values are obtained in large s_m region, the chip area increases. Also, the J/Y_0 are simulated and measured in the same method, where Y_0 (=1/Z_0) is 0.02S.

Figure 5 shows the EM-simulation results of the d_i and s_i dependence on J-inverters.

2.3 Design of the *K*-Inverter by Evaluating the Kinetic Inductance in the YBCO Film

In order to investigate the kinetic inductance of the K-inverter, we fabricate the YBCO $\lambda/2$ resonator connected with K-inverters and measure these effects. Figure 6(a) shows the transmission line model of the $\lambda/2$ resonator with K-inverters. Z_{0in} and Z_{0out} are source and load impedance, respectively. Because K-inverters are connected to the ground plane, $\lambda/2$ transmission line is transformed into the

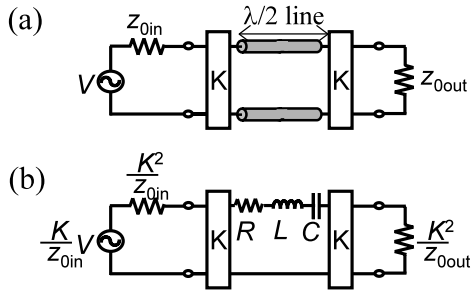

Fig. 6 $\lambda/2$ transmission line model (a) and equivalent circuit model of the resonator (b) connected with the K-inverters.

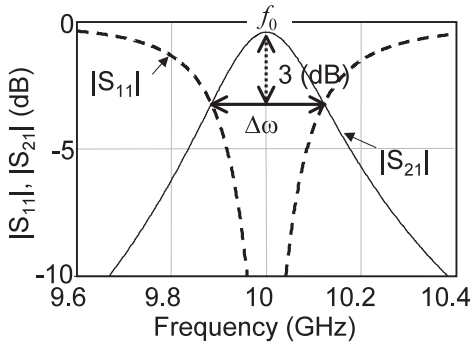

Fig. 7 Typical transmission characteristics of the resonator for K value estimation (EM-simulation results).

series resonator (R, L and C) at resonant frequency as shown in Fig. 6(b).

Figure 7 shows the EM-simulation results of typical transmission characteristics of the resonator for K value estimation. As shown in Fig. 6(b), input and output impedances are inverted with K-inverters.

An available power from the source (P_{av}) is given by,

$$P_{av} = \frac{|V|^2}{8Z_{0in}}. \tag{4}$$

When a power delivered to the load (Z_{0out}) is P_{out}, the ratio of the power (P_{out}/P_{av}) at f (=$\omega/2\pi$) is given by

$$\frac{P_{out}}{P_{av}} = |S_{21}(\omega)|^2 = \frac{\left.\frac{P_{out}}{P_{av}}\right|_{\omega=\omega_0}}{1 + Q_L^2\left(\frac{\omega}{\omega_0} - \frac{\omega_0}{\omega}\right)^2}, \tag{5}$$

$$\left.\frac{P_{out}}{P_{av}}\right|_{\omega=\omega_0} = |S_{21}(\omega_0)|^2 = \frac{4\frac{K^2}{Z_{0in}}\frac{K^2}{Z_{0out}}}{\left(\frac{K^2}{Z_{0in}} + R + \frac{K^2}{Z_{0out}}\right)^2} = \frac{4Q_L^2}{Q_{e1}Q_{e2}}, \tag{6}$$

where, the loaded quality factor (Q_L) is calculated form the unloaded quality factor (Q_u) and external quality factor (Q_{e1} and Q_{e2}), and are given by

$$Q_L \equiv \frac{1}{1/Q_{e1} + 1/Q_u + 1/Q_{e2}} = \frac{x}{K^2/Z_{0in} + R + K^2/Z_{0out}}, \quad (7)$$

$$Q_u \equiv \frac{\omega_0 L}{R} = \frac{x}{R}, \quad (8)$$

$$Q_{e1} \equiv \frac{\omega_0 L}{K^2/Z_{0in}} = \frac{x}{K^2/Z_{0in}}, \quad (9)$$

$$Q_{e2} \equiv \frac{\omega_0 L}{K^2/Z_{0out}} = \frac{x}{K^2/Z_{0out}}. \quad (10)$$

When $Z_{0in} = Z_{0out} = Z_0$, we can approximate $Q_{e1} = Q_{e2} = Q_e$. Finaly, Q_L, Q_u, Q_e and K are given by

$$Q_L = \frac{\omega_0}{\Delta\omega}, \quad (11)$$

$$Q_u = \frac{Q_L}{1 - |S_{21}(\omega_0)|}, \quad (12)$$

$$Q_e = \frac{2Q_L}{|S_{21}(\omega_0)|}, \quad (13)$$

$$K = \sqrt{\frac{Z_0\pi}{2Q_e}}. \quad (14)$$

We can calculate the K value from the transmission coefficient ($|S_{21}|$).

3. Results and Discussion

3.1 Experimental Results of K-Inverter

Figure 8 shows the photograph of the YBCO CPW $\lambda/2$ resonator connected with K-inverters. In order to improve the accuracy of the RF signals, the air coplanar probes (Cascade Microtech, GSG-150) touched the YBCO transmission line (see Fig. 8). The width of the signal line and gap interval is 60 μm and 26 μm. The meander interval of the $\lambda/2$ resonator is 300 μm. Figure 9 shows the photograph of the K-inverter. There were fabricated 2 types of the meander inductor (n=6, d_m=150 μm and 200 μm). Theses resonators are placed in a vacuum chamber with refrigerator cooling system. We measured the S parameters by a GP-IB controlled vector network analyzer (HP, HP8722C).

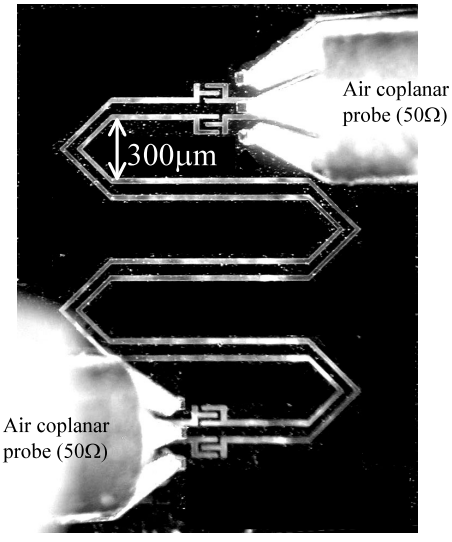

Fig. 8 Photograph of the YBCO CPW $\lambda/2$ resonator with probs.

Figure 10 shows the frequency response of the $|S_{21}|$ of the 2 resonators named #1 and #2 at 20 K. We can calculate the K values by using Eqs. (11)–(14). Table 1 shows the normalized K values from the experimental results, where Z_0=50 Ω. Experimental results are approximately 50% as large as that of the simulation results. This EM simulatior cannot evaluate the kinetic inductance (L_k) of the YBCO meander inductor, namely it is considered only a magnetic inductance (L_m). However, the experimental results ($L_{\rm exp}$) include L_k and given by,

$$L_{\rm exp} = L_m + L_k. \quad (15)$$

It is considered that the effect of the kinetic inductance of HTS appears conspicuously because the microwave current concentrates on the thin, narrow and long meander inductor (K-inverter section). Because L_m/L_k increases during the

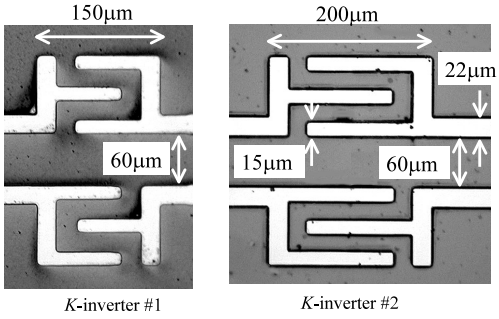

Fig. 9 Photograph of the K-inverters.

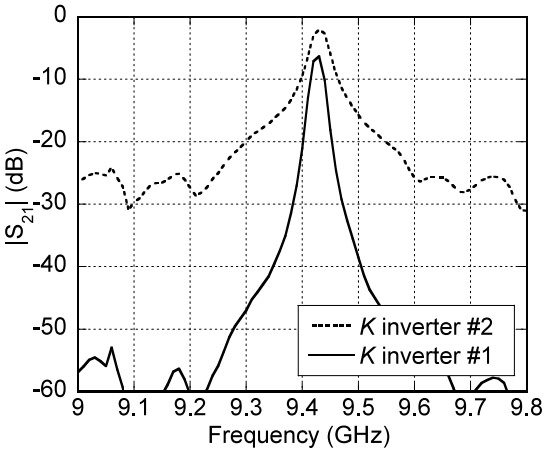

Fig. 10 Transmission characteristics of the resonators at 20 K.

Table 1 Normalized K values of the inverters.

K inverters	K/Z_0 (Sim.) (A)	K/Z_0 (Exp.) (B)	A/B (%)
K inverter #1	0.0291	0.0667	43.64
K inverter #2	0.0358	0.0701	50.98

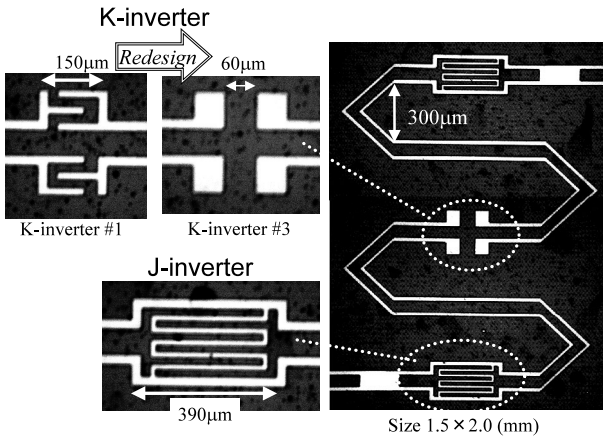

Fig. 11 Photograph of the prototype YBCO BPF with CPW $\lambda/4$ resonator (center frequency = 10 GHz, 2-pole, bandwidth = 1.5%).

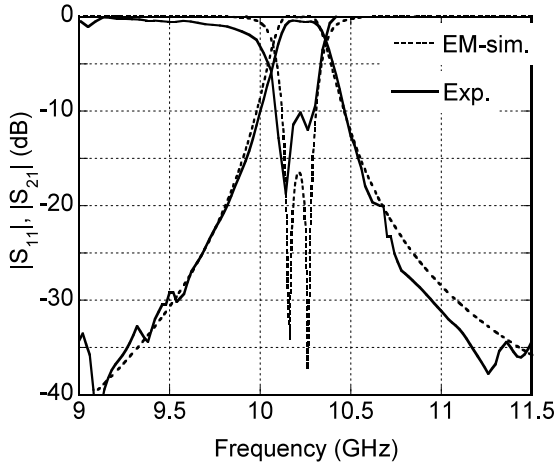

Fig. 12 Frequency response of the prototype YBCO CPW $\lambda/4$ resonator BPF at 20 K.

miniaturization, and L_k changes by the geometry factor, it is necessary to obtain the L_{exp} for fabricating $\lambda/4$ resonator BPF.

3.2 Experimental Results of a Prototype YBCO BPF

Figure 11 shows the photograph of the prototype YBCO BPF with $\lambda/4$ resonator for 10 GHz application (2-pole, bandwidth=1.5%). Using the experimental results of the inverters, we redesign the shape of the inverters by evaluating the kinetic inductance. In the figure, the meander inductor and interdigital gap are also shown. The filter size is 1.5×2.0 mm. We also modified the shape of the *K*-inverter as above process. The desirable K value is $K/Z_0 = 0.0291$ ($d_m = 150\,\mu$m), which is realized by the *K*-inverter #1 in the EM simulator (without evaluating the L_k), however, actual K value is realized by *K*-inverter #3 which has not the meander shape as shown in Fig. 11.

Figure 12 shows the frequency responses of the 2-pole YBCO CPW $\lambda/4$ BPF at 20 K. In the figure, broken lines show the S parameters of the EM simulation results. Because we evaluate the actual K values of the inverter experimentally, and redesign and fabricate the BPF, the bandwidth is almost similar to that of the EM simulation results.

4. Conclusion

K-inviter, which composed of a meander-shape inductor, is effective for the HTS microwave devices because of the extremely high quality factor. However, the effect of the kinetic inductance increases, as HTS BPF has thin, narrow and long transmission lines. We can design and fabricate the miniaturized YBCO CPW quarter-wavelength resonator BPF by experimentally evaluating the kinetic inductance of the *K*-inverter.

Acknowledgments

This work was supported in part by the Grant-in-Aid for Encouragement of Young Scientists (B) from the Japan Society for the Promotion of Science (JSPS). This work was partly supported by a grant of Fukuoka project in the Cooperative Link of Unique Science and Technology for Economy Revitalization (CLUSTER) of Ministry of Education, Culture, Sports, Science and Technology (MEXT).

References

[1] G. Tsuzuki, M. Suzuki, and N. Sakakibara, "Superconducting filter for IMT-2000 band," IEEE Trans. Microw. Theory Tech., vol.48, no.12, pp.2519–2525, Dec. 2000.
[2] J.S. Kwak, J.H. Lee, J.P. Hong, S.K. Han, W.S. Kim, and K.R. Char, "Narrow passband high-temperature superconducting filters of highly compact size for personal communication service applications," IEEE Trans. Appl. Supercond., vol.13, no.1, pp.17–19, March 2003.
[3] W. Hattori, T. Yoshitake, and K. Takahashi, "An HTS 21-pole microstrip filter for IMT-2000 base stations with steep attenuation," IEEE Trans. Appl. Supercond., vol.11, no.3, pp.4091–4094, Sept. 2001.
[4] K. Satoh, T. Mimura, S. Narahashi, and T. Nojima, "Today and tomorrow of HTS technology applications," MWE Microwave Workshop Digest, pp.102–117, 2000.
[5] H. Kanaya, T. Shinto, K. Yoshida, T. Uchiyama, and Z. Wang, "Miniaturized HTS coplanar waveguide bandpass filters with highly packed meanderlines," IEEE Trans. Appl. Supercond., vol.11, no.1, pp.481–484, March 2001.
[6] H. Kanaya, Y. Koga, T. Shinto, and K. Yoshida, "Design and performance of miniaturized HTS coplanar waveguide bandpass filters with highly packed meanderlines," IEICE Trans. Electron., vol.E85-C, no.3, pp.708–713, March 2002.
[7] H. Kanaya, J. Fujiyama, R. Oba, and K. Yoshida, "Design method of miniaturized HTS coplanar waveguide bandpass filters using cross coupling," IEEE Trans. Appl. Supercond., vol.13, no.2, pp.265–268, June 2003.
[8] G. Matthaei, L. Young, and E. Jones, Microwave Filters, Impedance- Matching Networks, and Coupling Structures, pp.427–440, McGraw-Hill, New York, 1964.
[9] H. Kanaya, K. Kawakami, F. Koga, Y. Kanda, and K. Yoshida, "Design and performance of miniaturized quarter-wavelength resonator bandpass filters with attenuation poles," IEEE Trans. Appl. Supercond., vol.15, no.2, pp.1016–1019, June 2005.

Haruichi Kanaya was born in Yamaguchi, Japan, in 1967. He received the B.S. (Physics) degree from Yamaguchi University in 1990, and the M.E. (Applied Physics) and D.E. degrees from Kyushu University in 1992 and 1994, respectively. In 1994, he became a Research Fellow (PD) of the Japan Society for the Promotion of Science. In 1998, he was a visiting scholar at the Massachusetts Institute of Technology (MIT), USA. He is currently engaged in the study and design of RF CMOS System LSI and superconducting microwave devices, as an Associate Professor in the Department of Electronics, Graduate School of Information Science and Electrical Engineering, and also System LSI Research center, Kyushu University. Dr. Kanaya is a member of the Institute of Electrical and Electronics Engineers (IEEE).

Koji Kawakami was born in Fukuoka, Japan, in 1980. He received the B.E. and M.E. (Electronics) degrees from Kyushu University in 2005. He was engaged in the study and design of superconducting microwave devices, as a M.E. student of the Department of Electronics, Graduate School of Information Science and Electrical Engineering, Kyushu University. He joined TOYOTA MOTOR Corporation in 2005.

Keiji Yoshida was born in Fukuoka, Japan, in 1948. He received the B.E., M.E. and Dr. Eng. degrees from Kyushu University in 1971, 1973 and 1978, respectively. He is currently engaged in the study of applications of superconducting thin films to microwave and optical devices and design of RF-LSI chips for SoC, as a Professor in the Department of Electronics, Graduate School of Information Science and Electrical Engineering, Kyushu University. Dr. Yoshida is a member of the Japan Society of Applied Physics.